Journal of Archaeological Science 176 (2025) 106167

Contents lists available at ScienceDirect

Journal of Archaeological Science

journal homepage: www.elsevier.com/locate/jas

Combining ATR far- and mid-infrared spectroscopy to distinguish native Australian plant exudates for cultural heritage analysis

Abigail K. Mann [a,b], Dominique Appadoo [c], Claire E. Lenehan [a,b], Rachel S. Popelka-Filcoff [d,b,*]

[a] Institute for Nanoscale Science and Technology, College of Science and Engineering, Flinders University, Bedford Park, South Australia, 5042, Australia
[b] College of Science and Engineering, Flinders University, Bedford Park, South Australia, 5042, Australia
[c] Australian Synchrotron, Clayton, Victoria, 3168, Australia
[d] School of Geography, Earth and Atmospheric Sciences, University of Melbourne, Melbourne, Victoria, 3010, Australia

ARTICLE INFO

Dataset link: Mann et al. Plant Exudates Mid-IR and Far-IR Data and Analysis (Original data)

Keywords:
Plant exudates
Pigment and stone binders
Synchrotron THz spectroscopy
Infrared spectroscopy

ABSTRACT

Native Australian plant exudates are an important material for a variety of cultural uses including hafting materials and pigment binders. Spectroscopic analysis of exudates informs on their composition, properties, use and conservation status. However, native Australian exudates are not as well characterized as European species, although there are often chemical parallels between the two. While mid-IR has been demonstrated as an effective and standard method to distinguish some key exudate species, the fingerprint-region characterisation can become challenging for a particular group of exudates due to spectral similarities or overlaps, and therefore discrimination is not easily achievable. Therefore, the complementary data on molecular interactions observed in the far-IR region can provide additional means to characterize and discriminate between genera. In this study, samples from European artist materials and native Australian exudates were studied by both laboratory-based mid-IR and synchrotron based far-IR. Results from this work include establishing a novel non-destructive far-IR method for plant exudates such as resins, gums and kinos on the molecular level, as well as multivariate statistical analysis to differentiate at both the genera and species level. These outcomes identify an innovative approach to understanding these complex molecular chemistries of plant exudates as well as a method to characterize resins, kinos and gums in important archaeological and cultural heritage materials in Australia and worldwide.

1. Introduction

People around the world have utilized plant exudates for a variety of cultural and technological uses across time and geographies, with traditions transversing across generations continuing into the present (Langenheim et al., 2003). Traditional uses of plant exudates around the world are the result of thousands of years of experimentation for the optimal procurement and use, where people initially harvested from local species and sources, however materials may also have been available via small and large exchange networks (Clarke, 2003, 2007; Nussinovitch, 2009). The majority of the species characterized in previous studies originally are from European and Mediterranean regions, with the plants since exported and cultivated in other regions of the world e.g. gum Arabic, colophony, manila copal, and gum elemi. (Prati et al., 2011; Vandenabeele et al., 2000).

However, there have been fewer investigations and characterization of plants and their exudates from Indigenous traditions in the archaeological record, particularly from Australia, North America, and sub-Saharan Africa, all of which have long-standing cultural and technological uses of plants and their exudates (Degano et al., 2018; Nussinovitch, 2009). For tens of thousands of years and as reflected through archaeological material, Indigenous Australians have traditionally used specific plant exudates for various applications, which also continue into present uses (Clarke, 2003, 2007; Langenheim et al., 2003). Specific materials and species are sought for their particular chemical and physical properties that lend them to optimized use in a variety of applications, including heating *Xanthorrhoea* exudates for the hafting of lithic materials (Maloney et al., 2015; Matheson and McCollum, 2014; Powell et al., 2013), adhering pigment particles together in bark paintings (Alcock, 2013; Blee et al., 2010; Matheson and McCollum, 2014; Reeves et al., 2013), and composing pigment binders and varnishes (Langenheim et al., 2003; Tworek-Matuszkiewicz, 2007). The

* Corresponding author. School of Geography, Earth and Atmospheric Sciences, University of Melbourne, Melbourne, Victoria, 3010, Australia.
E-mail address: rachel.popelkafilcoff@unimelb.edu.au (R.S. Popelka-Filcoff).

https://doi.org/10.1016/j.jas.2025.106167
Received 30 August 2024; Received in revised form 23 January 2025; Accepted 2 February 2025
Available online 17 February 2025
0305-4403/© 2025 The Authors. Published by Elsevier Ltd. This is an open access article under the CC BY license (http://creativecommons.org/licenses/by/4.0/).

cultural and practical uses capitalize on the fundamental chemistry of the exudate, which determines its properties (Georgiou et al., 2022).

1.1. Plant exudate chemistry

Several terms (such as resin and gum) are used inconsistently in the literature to describe these materials; therefore, for the purpose of this work, the term plant exudate is used to refer to any matter that has been excreted or extracted from the plant that can be solid or liquid (Matheson and McCollum, 2014). Resins are defined as being mixtures of volatile and non-volatile terpenoid and or phenolic secondary compounds which are lipid soluble (Alcock, 2013; Langenheim et al., 2003). *Eucalyptus* and *Corymbia* differ and are referred to as "kino" as they are dominated by phenolic and other aromatic constituents (Alcock, 2013; Langenheim et al., 2003). Gums documented from genera including *Araucaria* and *Callitris* are more predominantly composed of carbohydrates, therefore making them soluble in polar solvents (Langenheim et al., 2003).

Araucaria and *Callitris* are used for varnishes as they are composed of non-volatile terpenoids (Langenheim et al., 2003). The terpenoid composition promotes water solubility, facilitating easy incorporation into pigments. Exudates from *Xanthorrhoea* are documented to be primarily used as a hafting agent. *Xanthorrhoea* exudate structure is primarily composed of phenols, which when heated and used as an adhesive, forms a cooled glassy material that is insoluble in water (Langenheim et al., 2003). Exudates from *Eucalyptus* plants are composed of a complex mixture of phenols and terpenoids. These properties lead to a diverse range of water solubility and adhesion to materials such as rock and bark, giving *Eucalyptus* versatile uses as both an adhesive and a binder. The variance in broader molecular composition in *Eucalyptus exudates* such as functional group attachment position, and relative size, ratio, and complexity of the carbon backbone gives rise to slight changes in solubility, adhesion and interaction between the binder and pigments or substrate for use in cultural heritage materials.

1.2. Plant exudate analysis

These differing chemistries and properties (e.g., terpenoid versus a polysaccharide) arise from the differences in the functional groups of each type of exudate and therefore easily distinguishable via lab-based IR spectroscopy (Blee et al., 2010; Daher et al., 2010; Georgiou et al., 2022; Kendix et al., 2009; Matheson and McCollum, 2014; Monnier, 2018; Piña-Torres et al., 2018; Prati et al., 2011; Vahur et al., 2016). Several approaches have been used for the characterization and analysis of plant exudates from European and Mediterranean contexts, however unanswered questions remain on the ability of spectroscopic techniques to differentiate between species within genera. Techniques include color reflectance, Raman, mid-infrared spectroscopy (mid-IR), gas chromatography mass spectrometry (GC-MS) and pyrolysis gas chromatography mass spectrometry (py-GC-MS) to inform on characteristics such as color and major composition (Ghisalberti and Godfrey, 1998; Graf et al., 2020; Matheson and McCollum, 2014; Reeves et al., 2013).

A few recent studies have analyzed native Australian plant exudates in the context of cultural heritage and objects in museum collections (Alcock, 2013; Georgiou et al., 2022; Matheson and McCollum, 2014; Reeves et al., 2013), however, these are not universally comprehensive across the diversity of hundreds of species found across Australia and therefore not representative of the diversity of exudates used in cultural heritage materials and other applications. Reeves et al. compared Australian to European materials and demonstrated differentiation of chemistry and genera using py-GC-MS (Reeves et al., 2013). Georgiou and Popelka-Filcoff et al. demonstrated a complementary approach using py-GC-MS, FT-IR and X-ray Raman (XRS) to fully characterize exudates from molecular fragments, functional groups, and atomic environments, however this study was limited to the analysis of ten samples from four genera. A recent study by Matheson et al. identified easy-access methods for characterization of plant exudates however, these methods are designed primarily for basic identification rather than high-resolution differentiation between genera and species (Matheson, 2022).

The combination of mid-IR and far-IR provides complementary analyses towards the investigation of large, complex molecules where the functional groups are the same or similar, by further probing the intermolecular effects in the far-IR region where these effects may be used to differentiate based on bonding environments (Prati et al., 2011). There are a few studies on the far-IR analysis of plant exudates, by Prati et al. and Kendix et al. where the authors demonstrated the differentiation of European exudate materials using both mid-IR and far-IR and multivariate statistics for cultural heritage materials (Kendix et al., 2009; Prati et al., 2011). A study by Vahur et al. suggested that far-IR may be able to distinguish between sub-categories of gums, resins and kino (Vahur et al., 2016).

This manuscript has several key aims towards the characterization and understanding of native Australian plant exudates, to both expand understanding on their functional groups and material characteristics, but also to determine novel analytical approaches for the study of plant exudates in archaeological and cultural uses. This work develops and combines methods for mid- and far-infrared for chemical characterization of Australian native plant exudates and evaluates the advantages and limitations for these techniques for cultural heritage applications, which can be applied in both Australian and worldwide contexts. Each of the IR ranges provides a complementary set of chemical data for the exudates with mid-IR providing functional group information and far-IR providing information on changes in vibrational state. Multivariate statistical analyses were examined for both mid- and far-IR to determine classification of exudates based on fundamental chemistry and genus. Finally, the integration of the mid- and far-IR data was used to identify the chemistry of the exudates at both the genus and the species level for archaeological and cultural heritage applications.

2. Materials and methods

2.1. Worldwide model samples

Modern representative samples of similar chemistries were obtained from commercial suppliers (Table 1). While these are not native Australian species, these materials provide an important comparison in terms of their related chemistries to extant studies and databases (Prati et al., 2011). Specimens from the same species in this work have been previously extensively studied in the literature, utilizing IR, py-GC-MS and GC-MS and nuclear magnetic resonance spectroscopy (NMR) (Georgiou et al., 2022; Ghisalberti and Godfrey, 1998; Lambert, et al., 2005, 2007, 2008, 2010, 2021; Prati et al., 2011; Reeves et al., 2013).

2.2. Australian samples

This study utilized a unique collection of specimens of plant exudates that were collected by unknown scientists at the turn of the 20th century, with most of the samples collected between 1876 and 1905. (Table 2) (Georgiou et al., 2022). This sample set provides a unique opportunity to understand a diversity of plant exudates which is representative of archaeological and museum collection materials. A recent study combined py-GC-MS, IR, and X-ray Raman of selected genera over 10 samples from this collection and from the South Australian Museum (Georgiou et al., 2022).

2.3. Sample preparation

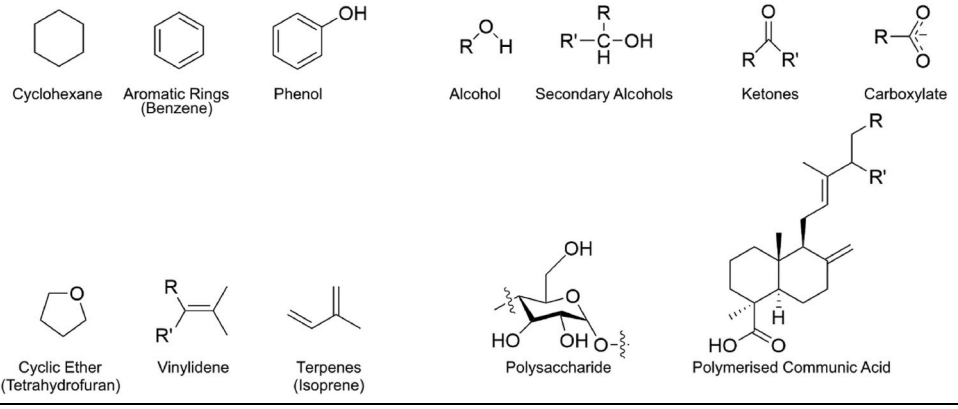
The natural Australian exudate samples and commercial samples were prepared by grinding a small amount (0.4g–2.0 g, depending on sample size) of the sample in an agate mortar and pestle until the formation of a fine, homogenous powder was observed. Based on prior

Table 1
Sample name, genus and species of the commercially available specimens used in the study.

Sample Name	Genus	Species	Manufacturer or Location	Main Chemical Components
Gum Sandarac	*Tetraclinis*	*articulata*	African sandarac tree	Polysaccharides, bicyclic and tricyclic diterpenes (Ghisalberti and Godfrey, 1998)
Copal Resin	Not listed	Not listed	TALAS, Brooklyn, New York	Bicyclic diterpenes
Gum Mastic	*Pistacia*	*lentiscus*	L. Cornelissen & Son, London England.	Pentacyclic Triterpenes
Colophony	Not listed	Not listed	Paintbox, Hahndorf, Australia (manufacturer not specified)	No literature information
Gum Damar	*Shorea* or *Hopea*	Not listed	Langridge Colors, Yarraville, Victoria.	Pentacyclic triterpenes

Table 2
Genus and major chemical composition of the Australian exudate specimens used in the study.

Genus	fUNCTIONAL GROUPS AND CHEMICAL COMPOSITION
A) XANTHORRHOEA	aromatic rings, ketones, alcohols
B) EUCALYPTUS	terpenes and phenolic compounds
C) Sterculia	polysaccharides, phenols, cyclic ethers
D) ACACIA	polysaccharides, aromatic compounds
E) MYOPORIUM	aromatic rings, cyclohexane rings, vinylidene, secondary alcohols
F) GREVILLEA	aromatic rings, carboxylates, ketones, cyclohexane rings
G) ERYTHROPHLEUM	polymerized communic acid, phenols
H) CANARIUM	polymerized communic acid, phenols
I) CALLITRIS	polymerized communic acid, phenols
J) ARACAURIA	polymerized communic acid
FUNCTIONAL GROUP STRUCTURES	



research, this study anticipated that the exudate material would not undergo chemical changes throughout the brief time interval and relatively benign conditions for analysis (Matheson and McCollum, 2014).

2.4. Mid-IR analysis of plant exudate (lab based IR)

Approximately 0.1 g of the prepared powders was analyzed using a ThermoFisher Scientific Nicolet Nexus 870 FT-IR (Fourier transform infrared) instrument (Waltham, Massachusetts, United States). The Thermo Smart Orbit™ (Bayly St, Mulwala, NSW) diamond ATR attachment was also utilized as a nondestructive alternative to transmission FTIR spectroscopy. The sample was deposited directly onto the ATR crystal, and the anvil was pressed into the loose powder to sufficient pressure to achieve the highest level of surface contact and analyzed using Nicolet OMNIC software. The analysis was undertaken with a deuterated triglycine sulfate (DTGS) detector and a KBr beam splitter. Samples were analyzed at optimized conditions of 4000-525 cm^{-1} with a resolution of 1 cm^{-1}. For each sample, 128 accumulated scans were recorded, with 128 background scans taken after every sample. Spectral analyses of three samples from the powdered exudate of the same species were analyzed, which demonstrated a notable correlation among the major peak positions observed across these samples. This approach facilitated the acquisition of a single spectrum for each sample in subsequent analyses.

2.5. Far IR analysis of plant exudates (synchrotron analysis)

Initial experiments determined that powdered samples were not optimized for far-IR due to insufficient signal and poor signal to noise ratio. To maximize sample to crystal contact for increased signal to noise in the far infrared region, approximately 0.1 g of the powdered sample was pressed without binder using 10 tonnes of pressure into a 13 mm circular disk using a standard die set and PIKE auto-crusher pellet press (Madison WI, USA). The pressed disk was then positioned on the ATR crystal for analysis. Spectra were acquired using Bruker IFS 125/HR Fourier Transform (FT) spectrometer, at the Australian Synchrotron THz Far Infrared beamline. The spectrometer was coupled with Pike Technologies Diamond ATR sampling accessory (6 μm) attachment, with a refractive index of 2.4 and a single bouncing refractive infrared beam with the angle of incidence at 45°. The samples were analyzed in the optimized range of 1000 cm^{-1} to 40 cm^{-1}. The resolution used was 4.0 cm^{-1}, using the mylar multilayer beam splitter. The aperture was 12.5 mm using a silicon bolometer detector. The source used was of synchrotron radiation with a beam current of 200.1 mA and a scanner velocity of 80.0 kHz at a temperature of 24.8 °C. A total of 1000 scans were run over each sample and each background, where an average spectrum was calculated overall (Blee et al., 2010; Edwards, et al., 1996, 2008; Prati et al., 2011).

2.6. Data processing and analysis

Data for absorbance versus wavenumber was plotted against each other for visual inspection, prior to being pre-processed using Bruker OPUS version 8.2.28. Initial visual inspection was undertaken, during which absorbance intensity peaks were identified using the single peak pick function. The spectra were then compared to literature spectra for each of the samples (Edwards, et al., 1996, 2008; Prati et al., 2011).

2.7. Mid-IR data analysis

The mid-infrared (mid-IR) data underwent several preprocessing steps prior to analysis. An ATR correction was applied using a refractive index (RI) of 2.418 (diamond). This was followed by baseline correction to reduce sloping effects in the data. The corrected spectra were then normalized to a range between 1 and 0. Spectral analysis and presentation was done using the resulting spectra in Origin Pro 9 version 9 E. Optimized spectral regions were selected for further analysis, specifically the ranges of 3500 cm^{-1}–2800 cm^{-1} and 1750 cm^{-1}–820 cm^{-1}.

Hierarchical cluster analysis (HCA) was conducted on the pre-processed mid-IR data using methods adapted from Blee et al., with the analysis performed in Unscrambler 10 (Camo Analytics, Norway). Principal component analysis (PCA) was also applied to the data to investigate patterns. The PCA analysis employed mean-centered single value decomposition (SVD) with cross-validation and included seven components. These analyses facilitated data exploration, outlier detection, graphical grouping, and the evaluation of spectral signal information.

2.8. Far-IR data analysis

For the far-infrared (far-IR) data, preprocessing included the subtraction of the average of five background scans from the sample spectra. The resulting absorbance spectra were normalized to a range between 0 and 1. The spectral region utilized for analysis was between 700 cm^{-1} and 50 cm^{-1}. A baseline correction was also applied to further enhance the quality of the data before statistical analysis.

Hierarchical cluster analysis (HCA) was performed on the far-IR data using 4–8 groups, with Euclidean distance as the metric and single linkage as the clustering method. HCA analysis was used to investigate initial categorization and linkages of the data. Principal component analysis (PCA) was then further employed on the same dataset, using a mean-centered single value decomposition (SVD) with cross-validation and using seven components. Similarly to the mid-IR data, PCA was used for pattern analysis, outlier detection, graphical grouping, and visualization of spectral information.

3. Results and discussion

3.1. Commercially available plant-based binders

Assessment of the validity of the methods for the laboratory-based ATR-FTIR and synchrotron-based far-IR was undertaken by comparing spectra for commercially available samples against similar specimens outlined by Prati et al. (Mann et al., submitted, Prati et al., 2011). Some spectral differences occur due to the fact that the Prati et al. data were not synchrotron-based and therefore are acquired at a lower resolution. Therefore the inherent differences in data quality and resolution as well as spectral range due to differences in instrumental configuration do not allow direct comparison of commercially available plant exudate data sets. (Prati et al., 2011). In addition, samples that are commercially available may go through unknown manufacturing processes with the addition of fillers and stabilizers which may interfere with the far-infrared signal of the plant exudate material. However, data from laboratory-based mid-IR can be more directly compared with the results from *Prati* et al. and are provided in the Data in Brief (Mann et al., submitted).

3.2. Laboratory based ATR-FTIR of natural plant exudates

Mid-IR spectra (Fig. 2) were obtained for exudates across 10 plant genera that have been documented to have historical significance. A more comprehensive set of mid-IR spectra were recorded and can be found in the Data in Brief (Mann et al., submitted). The spectra in the figure are representative of the majority of the spectra recorded across the genera examined.

The infrared absorption spectra showed variation between the ten genera. The spectra corresponding to the exudates from *Eucalyptus* (B), *Sterculia* (C) and *Acacia* (D) had common peaks that related to structural similarities in the chemical composition of the exudates. It was observed that the exudates' main components consisted of polysaccharides prominently described by a large OH peak (3300–3200 cm^{-1}), with low-intensity absorption peaks at 2918-3000 cm^{-1} (C-H stretching) from saturated and unsaturated carbon backbone structure. Many differences occur within the spectra allowing for distinction between the genera outlined. The main difference that is observed between the spectra from the *Eucalyptus* genera is the larger peak at 1605 cm^{-1} in comparison to the peak at 2982 cm^{-1} (conjugated C=C, 1605 cm^{-1}). This result could indicate the presence of ring structures indicating a phenolic resin which would then further be suggested by peaks present at 1445 cm^{-1} (aromatic ring stretching), 1311 cm^{-1} (phenol), 1191 cm^{-1} (phenol stretching) and possibly 1096 cm^{-1} which indicates the presence of cyclic C-O stretching in the form of large ring structures and or cyclic ethers. The transition peak at 1694 cm^{-1} could indicate the presence of a conjugated carboxylic acid, considering the shift in wavenumber to a lower frequency from the non-conjugated carboxylic acids.

The spectra for *Erythrophleum* (G), *Canarium* (H), *Callitris calcarata* (I) and *Araucaria* (J) were similar. The spectra for the exudate from the *Erythrophleum* genus showed a broad peak with a relatively low absorbance value in comparison to the larger absorbance values for the CH methyl stretching which occur at 2925 cm^{-1} and 2872 cm^{-1} with shoulders for each suggesting the are several different environments affecting the energy transition of the stretching. For *Callitris calcarata* (I) and *Araucaria* (J) there are distinct peaks at 3080 cm^{-1} (alkenes) differentiating them from *Erythrophleum* (G), and *Canarium* (H). There is a large broad unsymmetric peak at 1705 cm^{-1} which indicates the presence of a carboxyl group, which due to the position indicates the presence of a ketone. There is also a broad peak around the 1500 cm^{-1} region which along with the selection of peaks between 910 cm^{-1} and 1084 cm^{-1} and 1452 cm^{-1} indicate aromatic ring functionality. There is a smaller peak at around 1162 cm^{-1} indicating an aromatic phosphine group. A peak at 1380 cm^{-1} also suggests that there are phenol compounds present but in a lower amount in comparison to the carbonyl peak. The IR spectra (H) for *Canarium* genus differs from the *Erythrophleum* genus as aromatic ring bands at 1454 cm^{-1} and phenol band at 1379 cm^{-1} is greater relative to the absorbance of the ketone transition bands at 1705 cm^{-1}.

The absorption spectra (I) in the mid-infrared range for *Callitris calcarata* demonstrated peaks at 3500 cm^{-1} to 3000 cm^{-1} (COOH), with a major peak at 1692 cm^{-1} with a shoulder peak of 1652 cm^{-1} suggesting distinct types of C=O (carboxylate salt) bonds, that could be in conjugation with each other or an alkene group. There are multiple peaks at 1466 cm^{-1} (CH), 1448 cm^{-1} (CH), 1029 cm^{-1} (cyclohexane ring vibrations – out of plane), 887 cm^{-1} (CH) and 790 cm^{-1} (C-C vibrations) suggesting a complex backbone of cyclohexane rings with a carboxylic acid functional group. Overall, this result suggests the presence of polycommunic acid and an absence of peaks relating to that of aromatic species. The sample also likely contains a characteristic component, callitrisic acid (4-epidehydro-abietic acid) (Georgiou et al., 2022). The absorption spectra (J) of the *Araucaria* exhibited some key differences at the position of the absorption peaks at 1231 cm^{-1} and 1151 cm^{-1} (phenol components, tertiary alcohol). The peaks in the IR

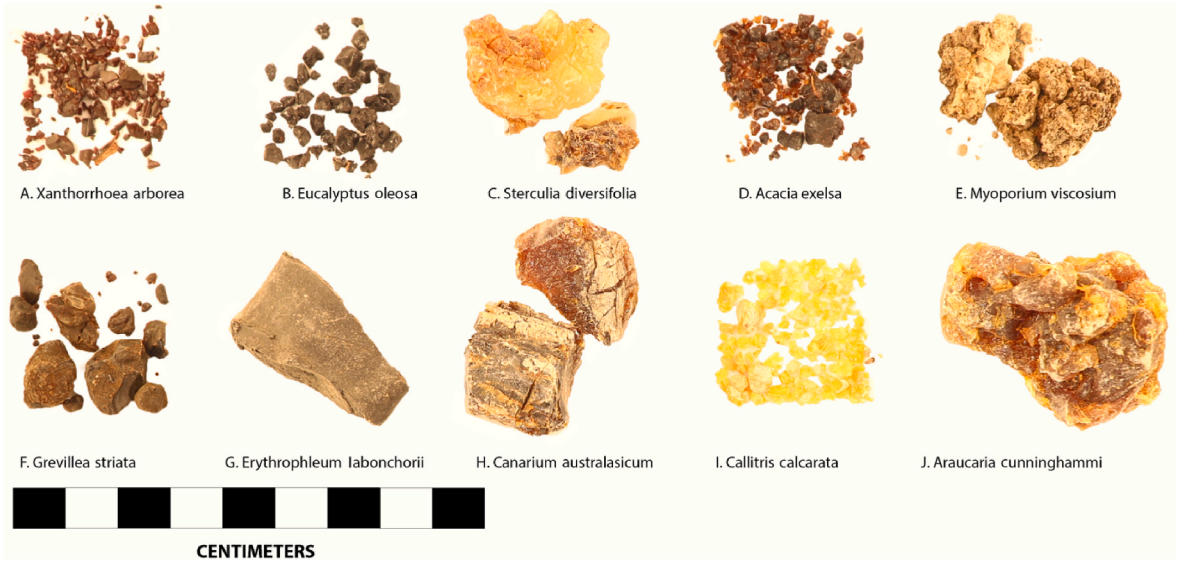


Fig. 1. Examples of the exudate bulk material from ten representative native Australian genera analyzed from the historic collection.

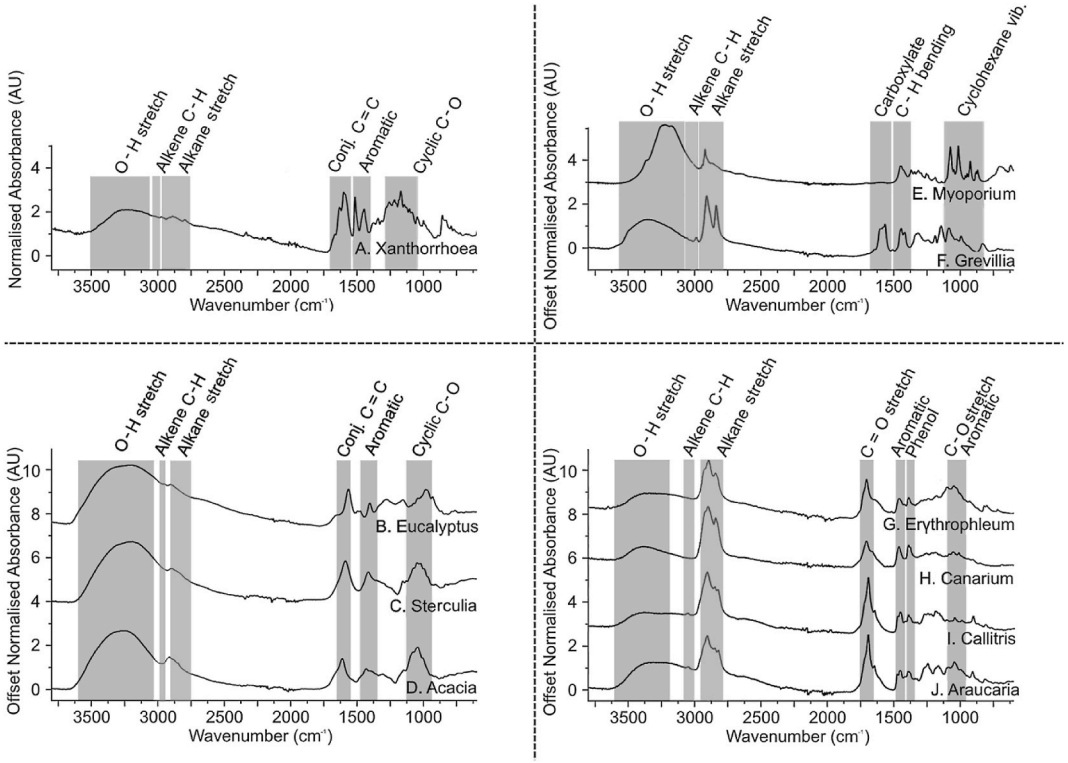


Fig. 2. Mid-infrared (3800-525 cm^{-1}) spectral analysis of the natural exudates of the showing the difference between genera in absorbance peak distribution of A) *Xanthorrhoea arborea*, B) *Eucalyptus oleosa*, C) *Sterculia diversifolia*, D) *Acacia exelsa*, E) *Myoporium viscosium*, F) *Grevillea striata*, G) *Erythrophleum laboncharii*, H) *Canarium australasicum*, I) *Callitris calcarata* and J) *Araucaria cunninghammi*.

spectra for the *Araucaria* species were broad at around both 1231 cm^{-1} and 1151 cm^{-1} in comparison to the three distinguishable peaks starting at 1260 cm^{-1} and a larger asymmetric peak at 1176 cm^{-1}. The peak at 1028 cm^{-1} (cyclohexane ring vibrations) is much greater for the *Araucaria*. There is also a broader extension of the peak at 1645 cm^{-1} which extends further into the 1500 cm^{-1} suggesting aromatic functionality and the presence of phenolic compounds.

The absorption spectra for the exudates collected from *Xanthorrhoea* (A), *Myoporium* (E) and *Grevillea* (F) had unique spectral features. *Xanthorrhoea* (A) contained multiple peaks around 1600 cm^{-1} (C=C), which suggests a broader distribution of energetic transitions due to multiple variations of chemical environments of the C=C functional group. There is a large distribution of weak peaks at 2850–3000 cm^{-1} (CH methyl) and 3000–3020 cm^{-1} alkenes for *Xanthorrhoea* and *Grevillea* which is an indication of a high complexity surrounding the carbon backbone. There is a strong peak at around 1512 cm^{-1}, suggesting aromatic groups which are absent in the other genera, supported by peaks at 1350-1000 cm^{-1} (aromatic skeletal vibrations) and 1631 cm^{-1} (conj. C=C). There is a broader peak at 3327 cm^{-1} which corresponds with OH stretching, and hence could indicate presence of an alcohol group, as there is the

absence of peaks at around 1690 cm^{-1} to 1710 cm^{-1}, indicating the absence of the polymerized communic acid related peaks in the far-IR spectra. NMR analysis by Ghisalberti and Godfrey show the resin from the *Xanthorrhoea* to contain mostly aromatic compounds (Ghisalberti and Godfrey, 1998). *Myoporium* (E) contained a large peak at 3270 cm^{-1} with an uneven distribution of peaks around the centre, which is observed by an asymmetric band with uneven weak shoulder on either side of the main peak. There is a large peak at around 2936 cm^{-1} (C-H asymmetric stretch) which suggests larger diversity in chemistry surrounding the main carbon atom (rings, longer carbon chains, shorter carbon chains) of methyl groups which is further supported by a series of peaks at 1456 cm^{-1} (CH bend), 1020 cm^{-1}, 967 cm^{-1}, 953 cm^{-1}, 929 cm^{-1} and 714 cm^{-1} (cyclohexane ring vibrations). The presence of bands at 1302 cm^{-1} (vinylidene C-H in plane bend) and 885 cm^{-1} (vinylidene C-H out of plane bend) further suggested the presence of a vinylidene group. The peaks ranging from 1322 cm^{-1} and 1350 cm^{-1} (C-H bending) suggest a smaller relative portion of the structure composed of methyne C-H groups. There is a band at 1081 cm^{-1} with a smaller band at approximately 1050–1060 cm^{-1} (C-O stretch) for a combination of primary and secondary alcohols. *Grevillea* (F) was observed to be highly complex but with a few defining bands including 1575 cm^{-1} (C=O carboxylate), 1326 cm^{-1} (CH bending)and strong peaks at 1611 cm^{-1} (conjugated ketone). There are minor peaks at slightly above 3000 cm^{-1} and 1650 cm^{-1} which suggest a minor portion of the molecule showing some unsaturation around the skeletal carbon background. Peaks at 2925 cm^{-1} and 2853 cm^{-1} (methylene C-H asymmetric/symmetric stretching) suggest a saturated carbon backbone, further supported by bands at 1452 cm^{-1}, 1427 cm^{-1} (methylene C-H) and between 1195 cm^{-1} and 1000 cm^{-1} suggesting a branched cyclohexane ring system.

The spectra *Sterculia diversifolia* (now *Brachychiton populneus)* is differentiated from others due to the small peak for a carbonyl group at 1731 cm^{-1} which suggests the presence of an aldehyde group. There is a strong peak at around 1592 cm^{-1} suggesting aromatic groups. There is also a large broad peak which centres at around 1034 cm^{-1} to 1012 cm^{-1}, composed of a range of peaks suggesting a complex aromatic and chain backbone structure. The minor peak for the aldehyde functional group at 1731 cm^{-1} (COH aldehyde) could be a result of oxidation of a primary alcohol group which could have occurred with aging of the exudate.

The spectra recorded for *Acacia bakeri* (Fig. 2D) showed distinct features such as large broad peak at 1595 cm^{-1} (carboxylate ions), 1412 cm^{-1} (carboxylates) 1284 cm^{-1} (aromatic ketones) 1123 cm^{-1} (1,2 disubstituted aromatic), 1052 cm^{-1}, 1017 cm^{-1} (1,2 disubstituted aromatic), 981 cm^{-1} (alkenes), 914 cm^{-1} (alkanes). This suggests that the resin is composed of aromatics, and polysaccharides which agrees with Granzotto, identifying pent5-oligosaccharide by mass spectrometry (Granzotto et al., 2019).

3.3. Synchrotron based far infrared of natural plant exudates

Often the peaks in mid-IR are convoluted due to multiple vibrational transitions that are difficult to differentiate as there are multiple placements of the same functional group within the molecule. This results in altered mid-IR peaks that overlap due to slight changes in the transition energies which reflect the different environments surrounding the functional groups in the large, complex molecules. By extending the spectral range to the far-IR region, additional data on the nature of intermolecular vibrations of functional groups such as aromatics and larger molecular assemblies can be obtained and therefore further

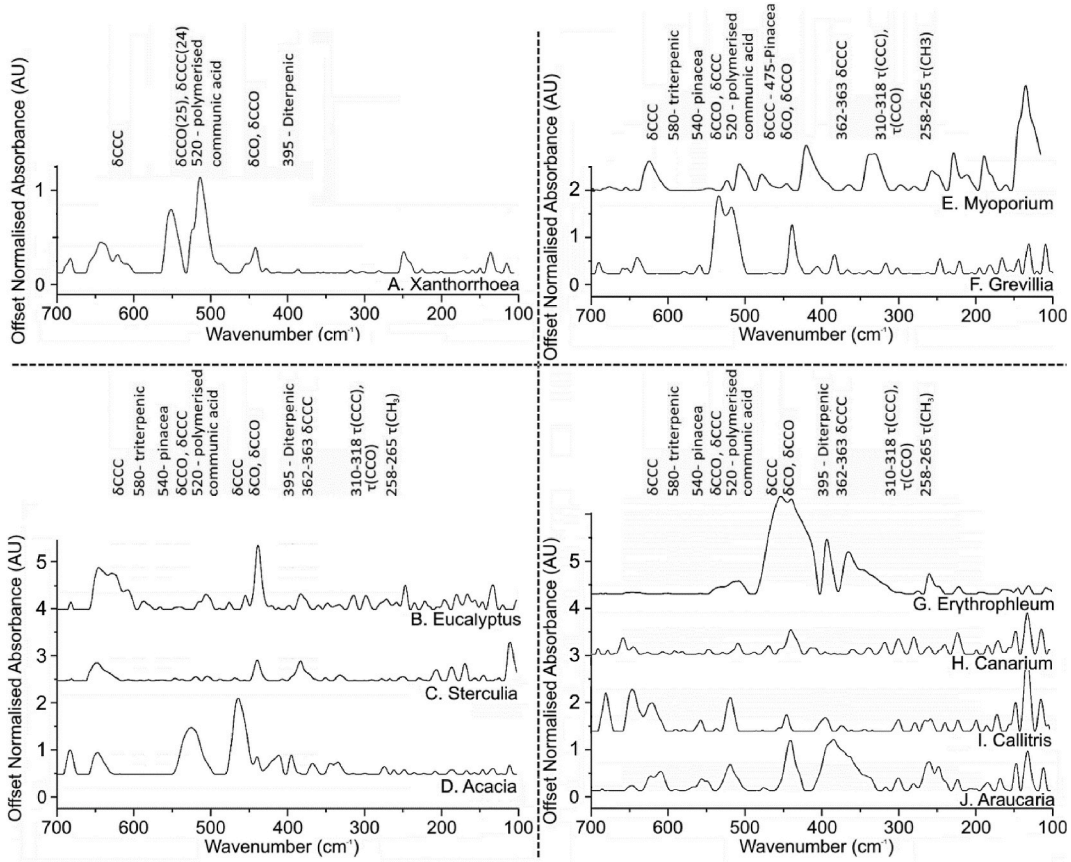


Fig. 3. Far-infrared (700-50 cm^{-1}) spectral analysis of the natural exudates of the showing the difference between genera in signal peak distribution of A) *Xanthorrhoea arborea*, B) *Eucalyptus oleosa*, C) *Sterculia diversifolia*, D) *Acacia exelsa*, E) *Myoporium viscosium*, F) *Grevillea striata*, G) *Erythrophleum labonchorii*, H) *Canarium australasicum*, I) *Callitris calcarata* and J) *Araucaria cunninghammi*.

differentiation between materials becomes possible (Ozaki, 2021).

Far-IR spectra as reported in Fig. 3, were obtained for exudates across 10 plant genera that have been documented to have historical significance and act as a representative collection showing a diversity of chemistry in the mixtures. The full far-IR spectra data set is in the Data in Brief article (Mann et al., submitted).

Some key intermolecular vibrations have previously been assigned in the literature such as δ CCC, δ CCO, tCH_3, t CH_3 -CH_2, δ CCC t CC, and ring deformations (Prati et al., 2011). However, some specific intermolecular vibrations cannot be assigned for each peak identified, however the overall spectral characterisation can be used to distinguish and differentiate genera due to their distinct chemistries. The benefit of with high resolution synchrotron-based far-IR data provides better signal to noise than laboratory-based instruments and therefore potentially clearer differentiation between sample types and chemistries.

A defining example for the complementary data from the far-IR is the mid-IR spectra for *Eucalyptus*, *Sterculia*, and *Acacia*. In the mid-IR, these spectra are visually indistinguishable, with *Eucalyptus* having minor differentiating peaks, therefore making the identification of an unknown from cultural heritage with this spectrum challenging to identify the genera based on mid-IR data alone. However, far-IR spectra identified that *Eucalyptus*, *Sterculia*, and *Acacia* contained a few key signature peaks and therefore intermolecular vibrations. The main defining transitions through the spectra collected from the *Eucalyptus* sample were 330 cm^{-1} and 500 cm^{-1}, not previously assigned to a transition, and a transition at 579 cm^{-1} which is a common peak for triterpenic resins. For the genus *Sterculia* main defining peaks were observed at 382 cm^{-1} (δ CCC), 351 cm^{-1}, 487 cm^{-1} (δ CCC) and 202 cm^{-1} and 164 cm^{-1}. The spectra for the *Acacia* sample exhibited broad peaks at 550 cm^{-1} and 360 cm^{-1} which in combination suggests the presence of at least a minor component being aromatic groups. These exudates could be primarily composed of highly branched polysaccharides which are suggested to have lower absorbance in the far infrared region (Vahur et al., 2016). Due to the low absorption of the main component, the resulting differentiation in peaks are likely due to differences in a smaller component of the complex molecules having a larger impact on the resulting spectra in the far infrared range.

Another example where additional data from far-IR provides further differentiation is genus *Callitris* and *Aracauria*, where the mid-IR spectra for the two exudates are not visually indistinguishable. Similarly to *Acacia*, the far-IR spectra for these samples exhibited common peaks at 556–558 cm^{-1} (δ CCO), 297 cm^{-1} – 299 cm^{-1} (t CCO), assigned by previous studies (Prati et al., 2011), with unassigned peaks of 517 cm^{-1}, 144 cm^{-1} and 129 cm^{-1}. Multiple peaks that were unique to the spectra, which provided differentiation between the genera, where the spectra for *Aracauria* had defining peaks at 261 cm^{-1} (tCH_3), 607 cm^{-1}, 383 cm^{-1} and *Callitris* exhibited peaks at 444 cm^{-1} (δ CCO), 255 cm^{-1} (t CH_3 -CH_2), 369 cm^{-1}, 387 cm^{-1} (δ CCC t CC) and 195 cm^{-1}. The spectrum showed some similar peaks to that of the far-IR spectra for pine resin provided through the LISA database such as 387 cm^{-1} (δ CCC t CC), and 387 cm^{-1} (δ CCC t CC) (Vahur et al., 2019).

Intermolecular vibrations in the far-infrared region are able to be further utilized to differentiate the complex molecular backbone structures in plant exudates where ring structures and lack of conjugation is present. The far-infrared region focuses on transition energies associated with lower energy vibrations and lattice vibrations than the mid-infrared region. This includes electronic transitions such as cyclic ring deformations (in and out of plane), rotation of the CH_3 group, torsional motions of the C-C-CH and COC groups and distortions in benzene and aromatic functional groups. Identification and the combination of these transitions, observable given the peak positions in the far-IR spectra, allows the differentiation for distinct types of ring deformation modes to become more apparent. For example, the spectra for *Myoporium* contains major peaks at 620 cm^{-1} (out of plane ring deformation), 501 cm^{-1} (out of plane ring deformation), 246 cm^{-1} (CH_3 rotation out of plane ring deformation) (Graf et al., 2020). These transitions are not identified in mid-IR, but far-IR gives more structural information on the complex carbon backbone of the material such as the orientation of ring structures, and diversity of connectivity between carbon chains and ring structures. Another example where far-IR can provide more insight on the different orientations of ring structures within the broader carbon-based backbone is the spectra for the genera *Grevillea*, which, contained peaks at 639 cm^{-1} (ring out of a plane bend, chair type deformation), 532 cm^{-1} (in-plane ring deformation C-C-CH torsion), 437 cm^{-1} (in-plane ring deformation), 405 cm^{-1} (not previously assigned) (Graf et al., 2020).

There are some well-defined transitions that have been established by Prati et al. and Graf et al. (Graf et al., 2020; Prati et al., 2011). The spectra of *Xanthorrhoea*, as seen in Fig. 3, is an example of the differentiating peaks being assigned to their chemistry, having differentiating absorption peaks at 510-508 cm^{-1} with a shoulder at 550 cm^{-1} (out of plane ring deformation), 439 cm^{-1} (in plane ring deformation) (δCO), 245 cm^{-1} (out of plane ring deformation CH_3 rotation), 619 cm^{-1} (out of plane ring deformation) and 633-635 cm^{-1} δ (CCC) across differing species (Graf et al., 2020). The number of peaks present, and the overall broadening of the peaks suggests a mixture of phenol/benzene components which have defined peaks in this region. *Erythrophleum* showed distinguishable features from other genera as it showed transitions that confirm the phenolic components to the resin, which have not been identified previously by far-IR for plant exudates. The peaks observed were 555 cm^{-1} (δ CCO), 513 cm^{-1} (not previously described), 453 cm^{-1} (aromatic), 392 cm^{-1} (benzene ring distortions), 364 cm^{-1} (δCCC) and 260 cm^{-1} (COC torsional), which identify aromatic and benzene ring distortions as well as information on the presence of the non-conjugated part of the structure.

There is a lack of literature regarding peak assignment in the far-IR region, which identifies the need to develop a database of far-infrared studies for plant exudates and related materials. An example of this is the spectra for genus *Canarium* which was difficult to interpret due to oscillations of low absorbance with two broader peaks centring at 525 cm^{-1} δ (CCO) and 297 cm^{-1}. Due to limited published data on the exact assignment of these peaks, it is difficult to identify specific transitions for specific peaks. However, far-IR probes deeper into the structural differences between the molecules identifying lower energy transitions such as in and out of plane ring deformation, torsional motion, rotational transitions in CH_3 groups and aromatic ring distortions.

3.4. Statistical analysis

Based on hierarchical cluster analysis as a preliminary analysis, PCA was then utilized to further identify potential patterns in the spectral data (Mann et al., submitted). Fig. 4 presents an overview of the findings for the PCA analysis in both the mid- and the far-IR.

3.5. Mid-IR statistical analysis

PC1/PC2 plots as observed in Fig. 4, differentiate four distinct chemical groups defined by the following main chemical base structures: *Callitris*: a resin containing a complex carbon ring structure and carboxylic acid component, *Xanthorrhoea*: resins with large aromatic components, *Acacia*: a exudate most likely a gum with large hydroxyl component in comparison to carbon backbone suggesting polysaccharide in nature and *Eucalyptus* which have higher portions of conjugated carbon backbone with phenols but higher diversity. Grouping is observed between species within some genera such as *Callitris* genera in both the mid- and far-IR data. *Xanthorrhoea* and *Eucalyptus* genera have higher amount of variance between the species (Fig. 4) where there is a greater spread in relation to the position of the data points, suggesting that there are greater differences in the spectra and therefore larger differences within each of the genera due to structural composition.

The variables that have the largest impact on the PC 1 for the mid-IR

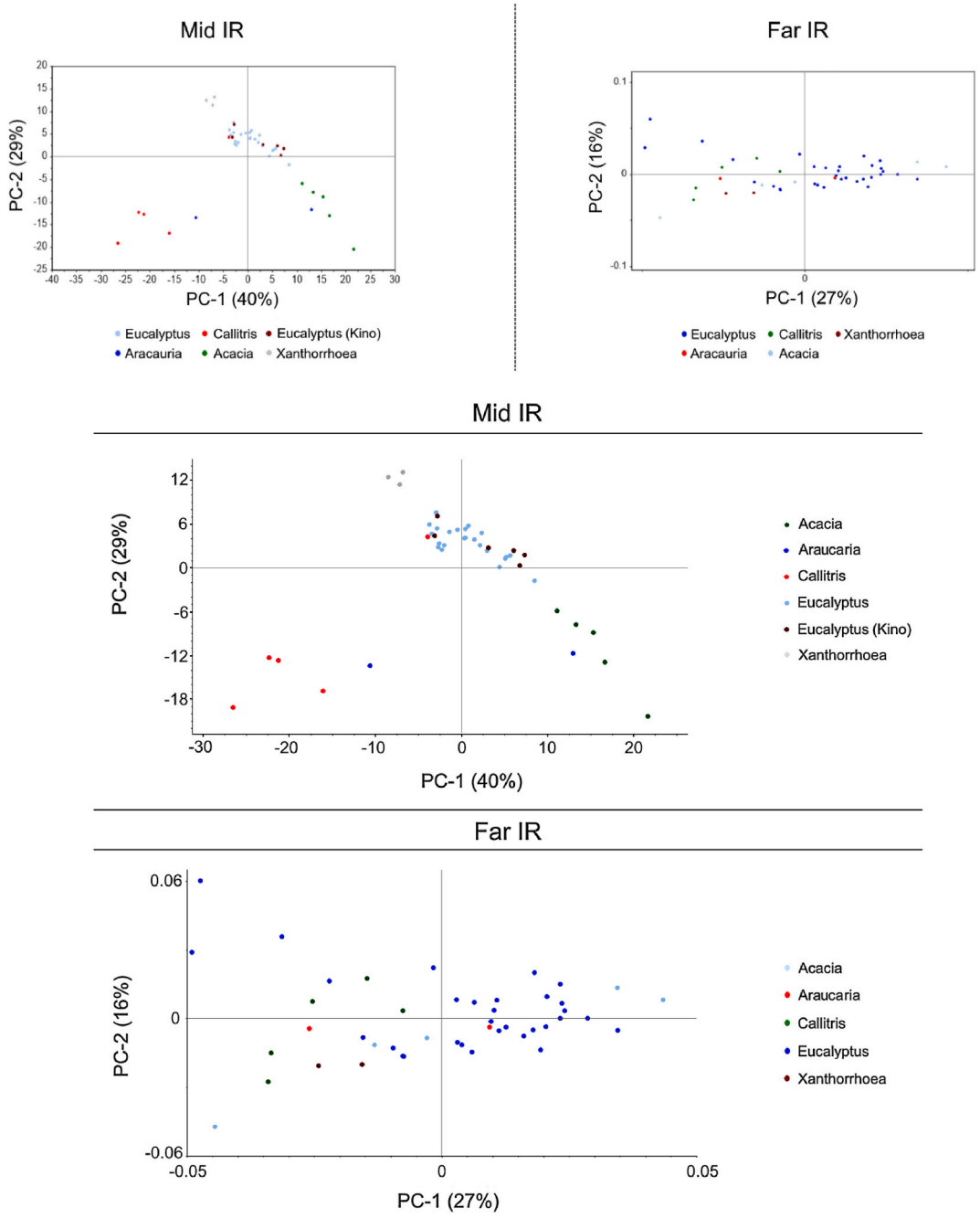


Fig. 4. Top: PCA scores for the mid-IR spectral data, bottom: PCA scores for the far-IR spectral data.

data, from the loadings are the wavenumbers between 3500 cm^{-1} and 3200 cm^{-1} (variation in OH stretching), 1730 cm^{-1} (variation in type of C=O group attachment and C=C) and 1640 cm^{-1}, 1260 cm^{-1} and 1170 cm^{-1}, 1090 cm^{-1} and 980 cm^{-1}. The main variables contributing to the variation in PC 2 are 1730 cm^{-1} to 1645 $cm^{-1,}$ 1601 cm^{-1}, 1515 cm^{-1}, and 1366 cm^{-1} to 1160 cm^{-1} and 1065 cm^{-1} to 882 cm^{-1}. Both *Callitris* and *Xanthorrhoea* show the greatest variation with this component between the two genera. The similarity is expected given that the spectra of the species within the genera for these show substantial similarities and are almost identical. There is separation between *Acacia*, *Eucalyptus* and *Xanthorrhoea* in the PC2 components but minor separation due to the variability in the PC–1 component.

Araucaria are outliers as the species *Bidwilli* shows more polysaccharide transition features similar to that of the *Acacia*, however, the *Cunninghammi* showed features similar to that of the *Callitris* resins where there are complex carbon ring structures with components being carboxylic acids but in relatively small quantities in comparison to the carbon backbone structures. Thus, through PCA analysis grouped the plant exudates by genera, that the exudate was chemically similar, however *Araucaria* has two types of exudates, both a resin and a gum and therefore this grouping is not an accurate comparison.

3.6. Far-IR statistical analysis

The spectra collected in the far-infrared, using synchrotron radiation, were observed to have inconsistent linear and curved baselines across the different spectra. Inconsistent baselines and global variation in intensity in ATR far-IR can be influenced by several factors, including inhomogeneities in particle size and accumulation of absorption peaks due to complex and diverse molecular structure such as chains of

polymeric resins (Lee et al., 2017). The data was pre-processed using a combination of methods to address baseline sloping and spectral intensity variations. A baseline correction (8–21 iterations) was used as a starting point, and then the spectra were normalized (1,0) as these are common techniques in preprocessing data. For both PCA and HCA analysis, the region between 700 and 50 cm^{-1} was used.

The principal component analysis of the far-infrared spectral data suggested differentiation using this data, between genera was not possible. The nature of the spread of data suggests that there is distinction between each species and the peak position and structure differs vastly with in each genus. This result can be attributed to the nature of the type of resin, for example whether it includes acid groups or aromatic groups, and degree of conjugation of the carbon-based backbone structure within the molecule. Loadings plots suggest that the main contributing wavenumber to the variance is around in the PCA analysis are for PC 1; 85 cm^{-1}, 249 cm^{-1}, 385 cm^{-1} (SCCC), 441 cm^{-1} (SCCO), 651 cm^{-1} contributing to the variance into the positive PC1 space, and 97 cm^{-1}, 117 cm^{-1}, 128 cm^{-1},243 cm^{-1}, 525 cm^{-1} (SCCO, SCCC polymerized communic acid) and 622 cm^{-1} which contributed variance into the negative PC1 space.

The separation in PC2 space in the positive region can be attributed to variation of peaks at wavenumber of 57 cm^{-1}, 82 cm^{-1} to 175 cm^{-1}, 240 cm^{-1} (CH_3 rotation), 261 cm^{-1} (CH_3 torsional motion). Presence and mobility of methyl groups indicating range of intermolecular interactions. The separation in the PC2 negative space can be attributed to wavenumbers of 645 cm^{-1} (out of plane ring vibrations), 510 cm^{-1}, 488 cm^{-1}, 444 cm^{-1} (SCCO).

Mid-IR data first has been able to differentiate between genus in most cases and this is further supported by groupings in PCA space. This identifies similar overarching chemical makeup throughout the species within a particular genus. To further differentiate between species, there is evidence that the far-infrared region due to its sensitivity to variation in intermolecular vibrations can be utilized and provides differentiation at a species level.

4. Conclusions and further research

This study demonstrated the effectiveness of infra-red spectroscopic investigation of complex aged cultural heritage materials in aged plant exudates to elucidate major functional groups and intermolecular interactions. By using mid-IR data and multivariate statistics, the native Australian genera could be differentiated through variation in key molecular structures which reflect distinct chemistries for each genus. Within each genus, further differentiation could be identified on the species level for the samples examined. Far-IR provided additional molecular structural information around ring structures and carbon backbones. Although the exact phenomena for each transition in the far-IR requires additional study, the quantified differences can be identified for the ten genera that were explored in this study and has potential to be used for additional exudates. Points of differentiation in the far-IR region are not as easily characterized as mid-IR and lack information to describe the exact peak assignment related chemistry, however as an initial study these results show an advantage of using far-IR in combination with mid-IR studies is that it provides more information of structural variation within the molecules.

Future work in this area includes identification of far-IR peaks by a combination of molecular modelling using density functional theory (DFT) with varying complexity of molecules, however this requires a considerable time investment for each identified molecular transition (Ennis et al., 2017). DFT can be used to simulate the infrared spectra for comparison with further experimental synchrotron-based studies of solid-state physical examples of the molecules (Ennis et al., 2017). The use of py-GC-MS analysis potentially provides more information on larger fragments within the exudates, when used in combination with IR spectroscopic data, which would provide a complementary technique.

By analysing the collection of aged plant exudates, his work also adds more data towards the identification of exudates in aged cultural heritage and archaeological materials from Australia. Many genera analyzed in this study are not in literature, and therefore this work will extend knowledge on the composition of these unique materials. In addition, these data will help to understand these complex materials and how to address conservation of cultural heritage materials that incorporate plant exudates from Australia and related chemistries worldwide.

CRediT authorship contribution statement

Abigail K. Mann: Writing – review & editing, Writing – original draft, Validation, Methodology, Investigation, Formal analysis. **Dominique Appadoo:** Writing – review & editing, Validation, Resources, Formal analysis. **Claire E. Lenehan:** Writing – review & editing, Methodology, Conceptualization. **Rachel S. Popelka-Filcoff:** Writing – review & editing, Writing – original draft, Supervision, Resources, Project administration, Methodology, Funding acquisition, Formal analysis, Conceptualization.

Declaration of competing interest

The authors declare the following financial interests/personal relationships which may be considered as potential competing interests: Rachel Popelka-Filcoff reports financial support and equipment were provided by the Australian Synchrotron. Rachel Popelka-Filcoff is on the editorial board of Journal of Archaeological Science. If there are other authors, they declare that they have no known competing financial interests or personal relationships that could have appeared to influence the work reported in this paper.

Acknowledgements

This research was undertaken on the THz–Far-Infrared beamline at the Australian Synchrotron, part of ANSTO.

The authors acknowledge Oliver Pring for his assistance at the Australian Synchrotron experiments, Professor Paul Kirkbride with the IR instruments, and Dr Jason Gascooke for his assistance with software analysis, both from Flinders University. The authors also acknowledge Professor Paul Kirkbride and Dr Paul Pigou for the transfer of the aged sample collection from Forensic Science South Australia (FSSA) to Flinders University. The authors also acknowledge Noa Abrahams for the photography and design assistance for Fig. 1.

Data availability

Mann et al. Plant Exudates Mid-IR and Far-IR Data and Analysis (Original data) (figshare)

References

Alcock, S., 2013. Painting Country: Australian Aboriginal artists' approach to traditional materials in a modern context. AICCM Bull. 34, 66–74.

Blee, A.J., Walshe, K., Pring, A., Quinton, J.S., Lenehan, C.E., 2010. Towards the identification of plant and animal binders on Australian stone knives. Talanta 82, 745–750.

Clarke, P.A., 2003. Australian Ethnobotany: an Overview, Australian Aboriginal Studies 2003, vol. 21.

Clarke, P.A., 2007. Aboriginal People and Their Plants, first ed. ed. Rosenberg Pub.

Daher, C., Paris, C., Le Ho, A.-S., Bellot-Gurlet, L., Echard, J.-P., 2010. A Joint Use of Raman and Infrared Spectroscopies for the Identification of Natural Organic Media Used in Ancient Varnishes, pp. 1494–1499.

Degano, I., Modugno, F., Bonaduce, I., Ribechini, E., Colombini, M.P., 2018. Recent advances in analytical pyrolysis to investigate organic materials in heritage science. Angew. Chem. Int. Ed. 7313.

Edwards, H.G.M., David, A.R., Brody, R.H., 2008. Fourier-transform Raman spectroscopy of archaeological resins. J. Raman Spectrosc. 39, 966–971.

Edwards, H.G.M., Farwell, D.W., Daffner, L., 1996. Fourier-transform Raman spectroscopic study of natural waxes and resins. Spectrochim. Acta Part A Mol. Spectrosc. 52, 1639–1648.

Ennis, C., Auchettl, R., Appadoo, D.R.T., Robertson, E.G., 2017. Density functional theory for prediction of far-infrared vibrational frequencies: molecular crystals of astrophysical interest. Mon. Not. Roy. Astron. Soc. 471, 4265–4274.
Georgiou, R., Popelka-Filcoff, R.S., Sokaras, D., Beltran, V., Bonaduce, I., Spangler, J., Cohen, S.X., Lehmann, R., Bernard, S., Rueff, J.-P., Bergmann, U., Bertrand, L., 2022. Disentangling the Chemistry of Australian Plant Exudates from a Unique Historical Collection, vol. 119. Proceedings of the National Academy of Sciences, e2116021119.
Ghisalberti, E.L., Godfrey, I.M., 1998. Application of nuclear magnetic resonance spectroscopy to the analysis of organic archaeological materials. Stud. Conserv. 43, 215–230.
Graf, W.F., Pearson, J.R., Appadoo, D.R.T., Robertson, E.G., Ennis, C., 2020. Synchrotron far-infrared spectra for the characterisation of molecular crystals of forensic interest: amphetamine, methamphetamine, MDA, MDMA and substituted methcathinones. Vib. Spectrosc. 110, 103115.
Granzotto, C., Sutherland, K., Arslanoglu, J., Ferguson, G.A., 2019. Discrimination of Acacia gums by MALDI-TOF MS: applications to micro-samples from works of art. Microchem. J. 144, 229–241.
Kendix, E.L., Prati, S., Joseph, E., Sciutto, G., Mazzeo, R., 2009. ATR and transmission analysis of pigments by means of far infrared spectroscopy. Anal. Bioanal. Chem. 394, 1023–1032.
Lambert, J., Santiago-Blay, J., Wu, Y., Contreras, T., Johnson, C., Bisulca, C., 2021. Characterization of phenolic plant exudates by nuclear magnetic resonance spectroscopy. J. Nat. Prod. 84.
Lambert, J., Wu, Y., Santiago-Blay, J., 2005. Taxonomic and chemical relationships revealed by nuclear magnetic resonance spectra of plant exudates. J. Nat. Prod. 68, 635–648.
Lambert, J.B., Heckenbach, E.A., Wu, Y., Santiago-Blay, J.A., 2010. Characterization of plant exudates by principal-component and cluster analyses with nuclear magnetic resonance variables. J. Nat. Prod. 73, 1643–1648.
Lambert, J.B., Santiago-Blay, J.A., Anderson, K.B., 2008. Chemical signatures of fossilized resins and recent plant exudates. Angew. Chem. Int. Ed. 47, 9608–9616.
Lambert, J.B., Wu, Y., Kozminski, M.A., Santiago-Blay, J.A., 2007. Characterization of Eucalyptus and chemically related exudates by nuclear magnetic resonance spectroscopy. Aust. J. Chem. 60, 862–870.
Langenheim, J.H., Markman, J., Thordarsen, G., 2003. Plant Resins : Chemistry, Evolution, Ecology, and Ethnobotany. Timber Press.
Lee, L.C., Liong, C.-Y., Jemain, A.A., 2017. A contemporary review on Data Preprocessing (DP) practice strategy in ATR-FTIR spectrum. Chemometr. Intell. Lab. Syst. 163, 64–75.
Maloney, T., Wood, R., O'Connor, S., Whitau, R., 2015. Direct dating of resin hafted point technology in Australia. Aust. Archaeol. 81, 35–43.
Mann, A.K., Appadoo, D., Lenehan, C.E., Popelka-Filcoff, R.S., Submitted. Mid- and far-infrared data for the analysis of Australian plant exudates. Data in Brief.
Matheson, C.D., 2022. Characterisation of the physico-chemical and optical properties of Australian native plant exudates for a simple method to determine archaeological resins and gums. J. Archaeol. Sci.: Report 42, 103360.
Matheson, C.D., McCollum, A.J., 2014. Characterising native plant resins from Australian Aboriginal artefacts using ATR-FTIR and GC/MS. J. Archaeol. Sci. 52, 116–128.
Monnier, G.F., 2018. A review of infrared spectroscopy in microarchaeology: methods, applications, and recent trends. J. Archaeol. Sci.: Report 18, 806–823.
Nussinovitch, A., 2009. Plant Gum Exudates of the World Sources, Distribution, Properties, and Applications. CRC Press, Boca Raton. Boca Raton.
Ozaki, Y., 2021. Infrared spectroscopy—mid-infrared, near-infrared, and far-infrared/terahertz spectroscopy. Anal. Sci. 37, 1193–1212.
Piña-Torres, C., Lucero-Gómez, P., Nieto, S., Vázquez, A., Bucio, L., Belio, I., Vega, R., Mathe, C., Vieillescazes, C., 2018. An analytical strategy based on Fourier transform infrared spectroscopy, principal component analysis and linear discriminant analysis to suggest the botanical origin of resins from Bursera. Application to archaeological Aztec Samples. J. Cult. Herit. 33, 48–59.
Powell, O., Fensham, R.J., Memmott, P., 2013. Indigenous use of spinifex resin for hafting in north-eastern Australia. Econ. Bot. 67, 210–224.
Prati, S., Sciutto, G., Mazzeo, R., Torri, C., Fabbri, D., 2011. Application of ATR-far-infrared spectroscopy to the analysis of natural resins. Anal. Bioanal. Chem. 399, 3081–3091.
Reeves, T., Popelka-Filcoff, R.S., Lenehan, C.E., 2013. Towards identification of traditional European and Indigenous Australian paint binders using pyrolysis gas chromatography mass spectrometry. Anal. Chim. Acta 803, 194–203.
Tworek-Matuszkiewicz, B., 2007. Australian Aboriginal bark paintings–their history, structure and conservation. Stud. Conserv. 52, 15–28.
Vahur, S., Teearu, A., Peets, P., Joosu, L., Leito, I., 2016. ATR-FT-IR spectral collection of conservation materials in the extended region of 4000-80 cm–1. Anal. Bioanal. Chem. 408, 3373–3379.
Vahur, S., Teearu, A., Peets, P., Joosu, L., Leito, I., 2019. Database of ATR-FTIR Spectra of Various Materials. https://spectra.chem.ut.ee.
Vandenabeele, P., Moens, L., Edwards, H.G.M., Dams, R., 2000. Raman spectroscopic database of azo pigments and application to modern art studies. J. Raman Spectrosc. 31, 509–517.